Supramolecular Polypseudorotaxane with Conjugated Polyazomethine Prepared Directly from Two Inclusion Complexes of β-Cyclodextrin with Tolidine and Phthaldehyde

Yu Liu,*,† Yan-Li Zhao,† Heng-Yi Zhang,† Xiao-Yun Li,† Peng Liang,† Xin-Zheng Zhang,‡ and Jing-Jun Xu‡

State Key Laboratory of Functional Polymer Materials for Adsorption and Separation, Department of Chemistry, Photonics Research Center Collage of Physics Science, Nankai University, Tianjin 300071, P. R. China

Received November 7, 2003; Revised Manuscript Received June 9, 2004

ABSTRACT: The supramolecular polypseudorotaxane (**3**) with π-conjugated polyazomethine is directly synthesized by the polycondensation of two simple inclusion complexes of β-cyclodextrin/*o*-tolidine (**1**) and β-cyclodextrin/*p*-phthaldehyde (**2**) and is comprehensively characterized by NMR, FTIR, circular dichroism spectra, powder X-ray diffraction, thermogravimetric (TG) and differential thermal analysis (DTA), scanning electron microscopy (SEM), and scanning tunneling microscopy (STM) both in solution and in the solid state. The results obtained have revealed linear microstructure of polypseudorotaxane **3** and different photophysical behavior as compared with the π-conjugated polyazomethine backbone (**4**). The present investigations prove a simple method for preparing supramolecular polypseudorotaxane by different complexes, which possess the potential to serve as molecular devices/machines and optical materials.

Introduction

Possessing a hydrophobic cavity, cyclodextrins (CDs) could be used as cyclic components to create the molecular machines with various molecular catenanes and rotaxanes/polyrotaxanes through the inclusion complexation with multifarious guest molecules, which are of special interest in molecular assembly.[1−10] Indeed, many nanometer-sized supramolecular assemblies were prepared by inclusion complexation of host CDs and guest molecules, which have been applied widely to molecular devices and molecular machines as well as functional materials, etc.[11−16] Recent investigations demonstrated that controlled intermolecular interactions are crucial to the exploitation of molecular semiconductors for both organic electronics and the viable manipulation and incorporation of single molecules into nanoengineered devices at a supramolecular level by threading a π-conjugated charge-transport macromolecule through CD rings.[17] More recently, Geckeler et al.[18] reported the preparation of fullerene-terminated soluble polyrotaxanes through the polycondensation in the presence of excess CDs. Farcas et al.[19] synthesized and characterized an aromatic polyazomethine with rotaxane architecture. On the other hand, investigations on the synthesis of π-conjugated polymers and their electronic, optoelectronic, and nonlinear optical properties have constituted a large area of research in contemporary polymer science.[20−23] However, the insulated polyrotaxanes of π-conjugated polymer prepared directly by the polycondensation of two ordinary inclusion complexes of β-CD with different guest molecules has rarely been studied so far to the best of our knowledge. Our recent investigations indicated that the polymeric rotaxane like the missing link could be fabricated from simple inclusion complexes of CDs and 4,4′-dipyridine molecules.[24] In present paper, we wish to report our results on the insulated polypseudorotaxane **3** with conjugated polyazomethine, by reaction of two different inclusion complexes, β-CD complex with *o*-tolidine **(1)** and β-CD complex with *p*-phthaldehyde (**2**), and using 2,4-dinitrofluorobenzene as the end-reaction agent. The binding behavior and structure of **3** were characterized by spectroscopic techniques in solution, powder X-ray diffraction studies, thermogravimetric (TG) and differential thermal analysis (DTA), scanning electron microscopy (SEM), and scanning tunneling microscopy (STM) in the solid state. The obtained results showed that the resulting complexes of β-CD with guest molecules are the key step for preparing conjugated polypseudorotaxane as insulated nanometer-sized wires. As compared with conjugated aromatic polyazomethine backbone **4**, the insulated polypseudorotaxane **3** displayed different photophysical behavior and longer fluorescence lifetimes, which will serve to further our understanding of this recently developing, but less investigated, area of suparmolecular chemistry and polymer science.

Results and Discussion

Synthesis. Insulated polypseudorotaxane **3** was prepared directly by the polycondensation of complexes **1** and **2** in *N*,*N*-dimethylformamide (DMF) solution and then added 2,4-dinitrofluorobenzene to complete the reaction, according to the procedures shown in Scheme 1. The studies on the CPK model of oligomers indicated that the size of 2,4-dinitrofluorobenzene is somewhat smaller than that of the cavity of β-CD, so the polymer **3** was called "polypseudorotaxane". During our experiments, the DMF solution of resultant mixture of complexes **1** and **2** was clear, but after adding the 2,4-dinitrofluorobenzene (liquid state), the precipitate of polypseudorotaxane was formed gradually, which indi-

† State Key Laboratory of Functional Polymer Materials for Adsorption and Separation, Department of Chemistry.
‡ Photonics Research Center Collage of Physics Science.
* Corresponding author: Tel +86-22-23503625; Fax +86-22-23503625; e-mail yuliu@public.tpt.tj.cn.

10.1021/ma0356717 CCC: $27.50
Published on Web 07/29/2004

Scheme 1. Schematic Representation of the Formation of 3 and 4

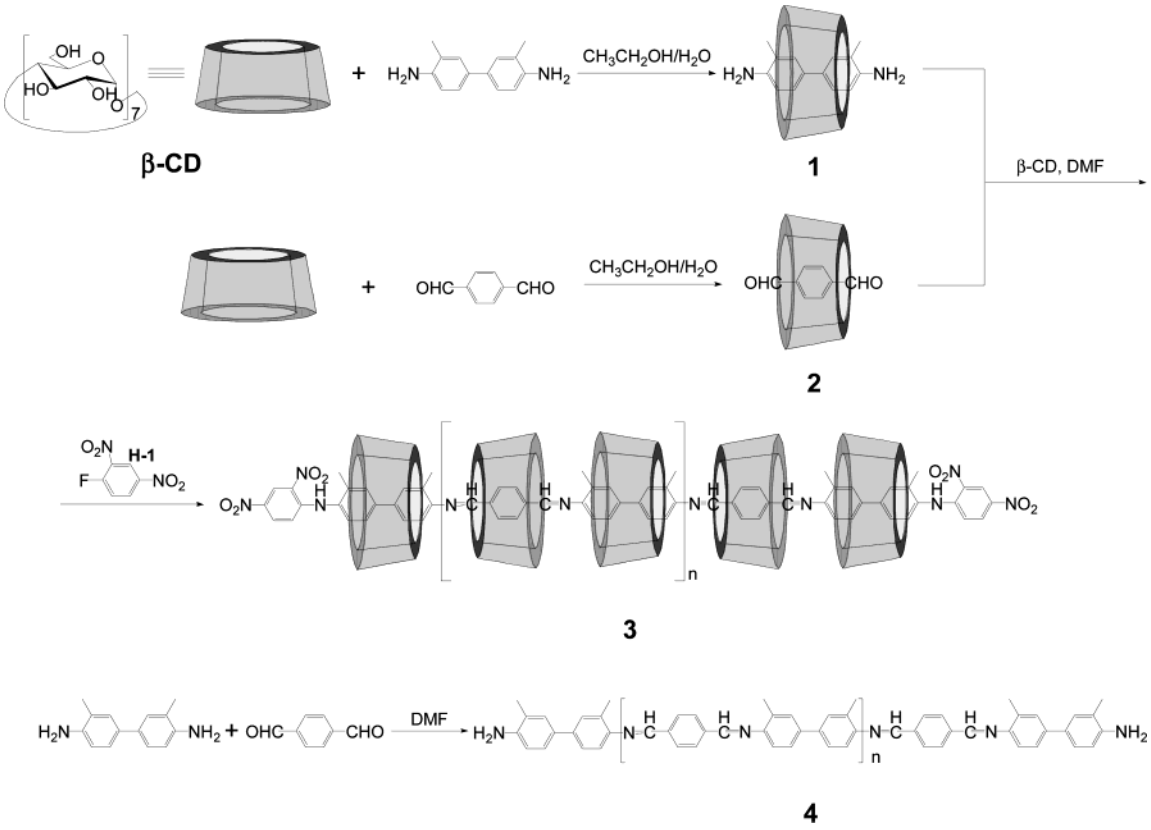

cated that polypseudorotaxane with 2,4-dinitrobenzene possess lower solubility in DMF. We also attempted to prepare a backbone compound of **3**, i.e., the polyazomethine polymer with the 2,4-dinitrobenzene end groups, but only obtained the polyazomethine polymer **4** without the end groups, which is attributed to the infusibility of **4** in traditional solvent (DMF, DMSO, CH_3OH, CH_3CH_2OH, CH_3CN, CH_3COCH_3, $CHCl_3$, H_2O, and so on), preventing the further reaction between the **4** and 2,4-dinitrofluorobenzene.

The feasibility of polycondensation would depend on the stability of the inclusion complexes **1** and **2** in DMF. Therefore, the titration experiments were performed using UV−vis spectrometry to demonstrate the stability of the inclusion complexes. In the titration experiments, the UV absorption maximum of *o*-tolidine (or *p*-phthaldehyde) is gradually decreased upon addition of varying amounts of *β*-CD in DMF at 25 °C. The results obtained indicated that the *β*-CD and *o*-tolidine **(**or *p*-phthaldehyde) form the 1:1 inclusion complexes, giving the binding constants of **1** ($K_S = 568 \pm 31\ M^{-1}$) and **2** ($K_S = 742 \pm 44\ M^{-1}$). We attempted initially to synthesize polypseudorotaxane **3** according to the concept by the condensing of *o*-tolidine and *p*-phthaldehyde in the presence of equimolar *β*-CD but did not succeed in getting the polypseudorotaxane. Interestingly, the polycondensation of inclusion complexes **1** and **2** in the presence of an excess of *β*-CD and then adding 2,4-dinitrofluorobenzene gave the polypseudorotaxane **3**. One reasonable explanation for this phenomenon is that a high *β*-CD concentration may induce the host−guest equilibrium transferring to form more complexes **(***β*-CD/*o*-tolidine and *β*-CD/*p*-phthaldehyde) in the reaction solution, which afford a good probability that the polycondensation reactions could take place between the amido group in *β*-CD−*o*-tolidine complex and the aldehyde group in *β*-CD−*p*-phthaldehyde complex to give the polypseudorotaxane **3**.

Crystal Structure of Complex 1. In context, direct evidence of inclusion complex **1** of *β*-CD with *o*-tolidine molecule has been obtained. As shown in Figure 1, the *o*-tolidine molecule in the crystal **1** (orthorhombic, *C*222(1))[25] is deeply included in *β*-CD cavity with a dihedral angle of 84.1° between the plane of the *o*-tolidine molecular axis and the heptagons composed of seven oxygen atoms of the *β*-CD and a dihedral angle of 34.3° between aromatic rings *a* and *b* of every *o*-tolidine molecule. Two *β*-CDs in a head-to-head dimer arrangement were connected by 11 hydrogen bonds from the hydroxyl groups on the secondary sides of the *β*-CDs. Especially, *π*−*π* interactions[26,27] between the *b* ring and the *a*′ ring with a dihedral angle of 1.4° and a centroid separation of 4.339 Å played crucial roles, which are infrequent in the crystal structures of the inclusion complexes between the CDs and guest molecules. (Among them, the centroid separation between the amino nitrogen atom in the *b* ring (or the *a*′ ring) and the *a*′ ring (or the *b* ring) is 3.580 Å.[28]) The head-to-head dimer can further self-assemble to form channel-type polymeric supramolecules through three hydrogen bonds between the dimers.

Polymerization Degree. It is a fact that the solubilities of **3** and **4** are too low in DMF to perform solution-phase NMR and GPC analysis. On the other hand, the Schiff base may be decomposed in the acidic environment to become dissoluble. To determine the repeat unit numbers in **3**, the ^1H NMR experiment was performed in DMSO-d_6−DCl mixture solution (DCl was added to the DMSO solution of **3** (0.8 g dm^{-3}) to make an acidic environment and control the pD value approximate to 5.0), and the spectrum of the decomposed units of **3** is obtained, as illustrated in Figure 2. From

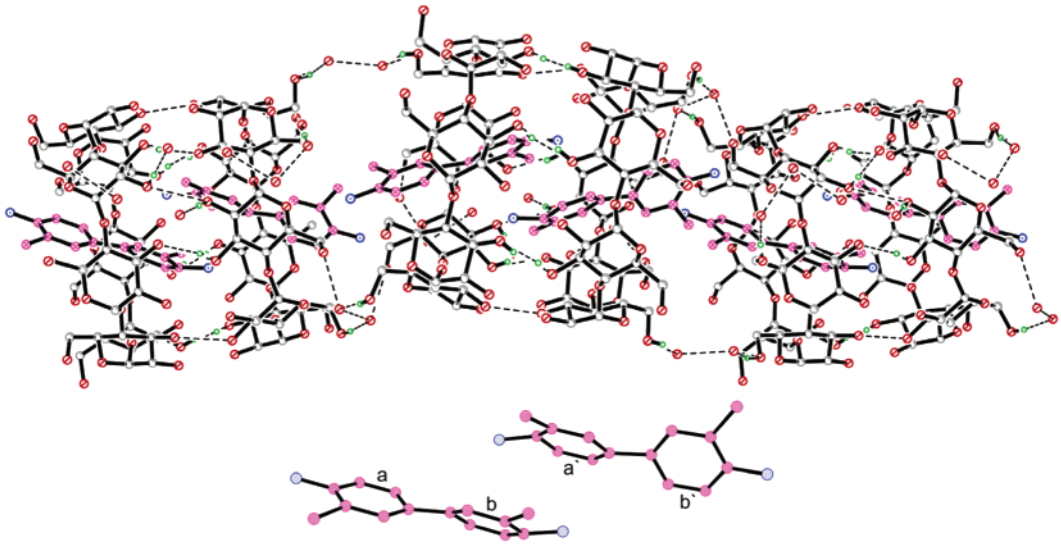

Figure 1. X-ray crystal structure showing the head-to-head channel structure of **1** (top) and *o*-tolidine backbones (bottom). *o*-Tolidine molecules are colored by atom type: blue, nitrogen atoms; pink, carbon atoms; black, chemical bonds. The *β*-CDs are also colored by atom type: gray, carbon atoms; red, oxygen atoms; green, hydrogen atoms involved in hydrogen-bonding interactions.

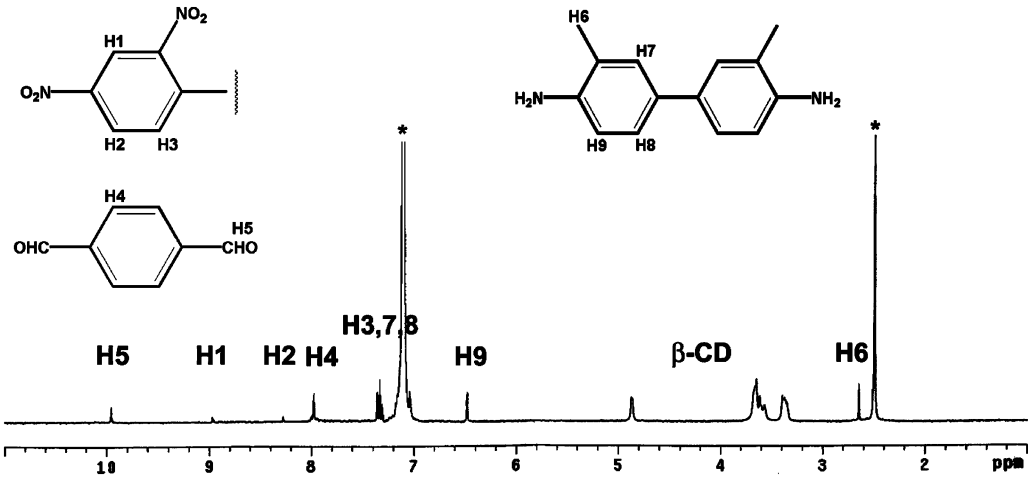

Figure 2. ^{1}H NMR spectrum of the decomposed units of **3** in DMSO-d_6−DCl mixture solution at 25 °C.

the ^{1}H NMR spectrum, a comparison of the area of proton peaks indicated that the ratio of every *o*-tolidine group's methyl protons (a molecule of *o*-tolidine contains six methyl protons, δ = 2.63 (s)) and *β*-CD protons (a molecule of *β*-CD contains 49 protons in DMSO-d_6−DCl) is 6.0:88.4, and the ratio of every *p*-phthaldehyde group's aromatic protons (a molecule of *p*-phthaldehyde contains four aromatic protons, δ = 7.95−7.98 (m)) and *β*-CD protons is 4.0:81.2. Consequently, the ^{1}H NMR data indicated approximatively that the polypseudorotaxane **3** has a structure with one *β*-CD ring for each azomethine link, and it is possible for some segments of azomethine devoid of any CD rings. Furthermore, the ratio of 2,4-dinitrofluorobenzene's H-1 proton (δ = 8.97 (s)) and *o*-tolidine group's methyl protons is 2.0:45.7 (equivalent to two 2,4-dinitrofluorobenzene moieties vs eight *o*-tolidine moieties), indicating that the *n* value of polypseudorotaxane **3** is about 3, i.e., ca. 9 *β*-CD rings in a polypseudorotaxane. In the ^{1}H NMR spectrum of **4** (0.7 g dm^{-3}) in DMSO-d_6−DCl mixture solution (pD ≈ 5.0), a comparison of the area of proton peaks showed that the ratio of *o*-tolidine group's methyl protons (δ = 2.66 (s)) and *p*-phthaldehyde group's aromatic protons (δ = 7.96−7.98 (m)) is 4.0:7.1, indicating that the *n* value of **4** is about 5 (containing about six *p*-phthaldehyde moieties and seven *o*-tolidine moieties). These results are also consistent with the theory prediction of Carothers' equation.

Furthermore, the *n* value was evaluated from the results of the elemental analysis of **3** and **4** by using eq 1 for **3** and eq 2 for **4**, respectively:

$$N\,(\%) = \frac{14.007(2n+8)}{n(2M_{CD} + M_{PH} + M_{TO}) + 3M_{CD} + M_{PH} + 2M_{TO-1} + 2M_{DI}} \times 100\% \quad (1)$$

$$N\,(\%) = \frac{14.007(2n+4)}{n(M_{PH} + M_{TO}) + M_{PH} + 2M_{TO-2}} \times 100\% \quad (2)$$

where M_{CD}, M_{PH}, and M_{DI} indicate the molecular weights of *β*-CD, *p*-phthaldehyde residue, and 2,4-dinitrofluorobenzene residue, respectively; M_{TO}, M_{TO-1}, and M_{TO-2} indicate the molecular weights of *o*-tolidine residue, *o*-tolidine terminal group in **3**, and *o*-tolidine terminal group in **4**, respectively. The numerator of equation contains the summation in atomic weight of all nitrogen atoms of the molecular assembly.[7b,29,30] From the equation, the values of *n* are obtained as 3

for polypseudorotaxane **3** and 6 for polymer **4**; correlative average molecular weights (MW) are about 12 001 and 2385, respectively.

NMR and FTIR Spectra. Usually, guest molecules included in CD cavities give rise to chemical shifts in ^{1}H NMR spectra.[5,12] Therefore, the binding behavior of complexes **1** and **2** in solution were evaluated by ^{1}H NMR spectroscopy at 25 °C in D_2O. For complex **1**, *ortho* (H^o) and *meta* (H^m) protons of *o*-tolidine in the presence of β-CD shift upfield about 0.26 and 0.10 ppm, respectively, and no chemical shift was found for methyl protons of *o*-tolidine, which reveal that the aromatic rings of *o*-tolidine molecule must be located on the interior of β-CD cavity but the all methyl groups outside the cavity. These results indicate that the inclusion mode of complex **1** observed in the solid state also exists in solution. Furthermore, all of aromatic protons of the *p*-phthaldehyde in complex **2** were shielded by about 0.01 ppm in the presence of β-CD, indicating that the *p*-phthaldehyde molecule and β-CD formed the inclusion complex.

The ^{13}C cross-polarization magic angle spinning (CP/MAS) and ^{1}H MAS NMR spectra of the inclusion complexes of β-CD with guest molecules in the solid state have been extensively studied by using the dipolar dephasing technique,[31−33] which yield more detailed analysis of the relationships between motion, structure, and mobility for several related series of guest molecules. Therefore, ^{13}C CP/MAS and ^{1}H MAS NMR spectra of **3** and **4** were obtained on a Varian UNITYplus 400 NMR spectrometer at 25 °C. From the ^{13}C CP/MAS NMR spectrum of **3**, signals at 61.3, 73.6, 83.6, and 103.4 ppm were assigned to the characteristic peaks of β-CD carbon atoms; signals at 118.8, 125.8, 130.8, and 139.4 ppm were ascribed to the characteristic peaks of phenyl carbon atoms; signals at 157.5 ppm were the characteristic peaks of azomethine (C═N) carbon atoms; and signals at 16.0 and 19.8 ppm were due to the methyl carbon atoms of *o*-tolidine moiety in **3**. From the ^{13}C CP/MAS NMR spectra of **4**, we also observed the characteristic signals of phenyl carbon atoms (118.9, 127.5, 131.0, and 139.3 ppm), azomethine (C═N) carbon atoms (157.3 and 160.9 ppm), and the methyl carbon atoms of *o*-tolidine (16.1 and 20.2 ppm). Furthermore, ^{1}H MAS NMR spectra showed three peaks at 2.47, 4.98, and 7.59 ppm for **4** but only one major characteristic peak at 2.70 ppm for **3**, and the broader resonances at the left of the sharp line correspond to the other two unresolved peaks, which indicated that the presence of β-CD in **3** shields the motion of protons and consequently makes the splitting of polyazomethine protons be masked. In the FTIR spectra, the characteristic absorption peaks of β-CD in **3** were shown at 3361 cm^{-1} (ν_{O-H}) and 1031 cm^{-1} (ν_{C-O-C}), and the absorption at 1622 cm^{-1} was due to the C═N stretching vibration. The C═N stretching vibration in **4** was at 1621 cm^{-1}, and the absorption peak of the amine end groups was detected at 3341 cm^{-1}.

ICD Spectra. To deduce the conformation of interaction between the achiral chromophoric compound and the β-CD chiral cavity, induced circular dichroism (ICD) spectra of **1**−**4** were measured. As can be seen from Figures 3 and 4, the circular dichroism spectrum of **1** showed a strong positive Cotton effect around 276 nm ($\Delta\epsilon$ = 3.24 dm^{-3} mol^{-1} cm^{-1}, in H_2O), and **2** showed a positive Cotton effect around 263 nm ($\Delta\epsilon$ = 1.59 dm^{-3} mol^{-1} cm^{-1}, in H_2O). Polypseudorotaxane **3** gave a major

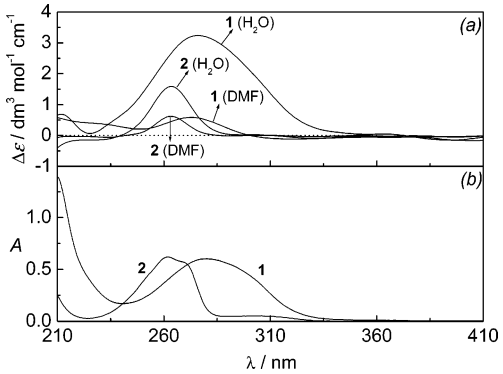

Figure 3. Circular dichroism (a) and absorption (b) spectra of complex **1** (3.2×10^{-5} mol dm^{-3}) and **2** (4.7×10^{-5} mol dm^{-3}) in aqueous or DMF solution at 25 °C.

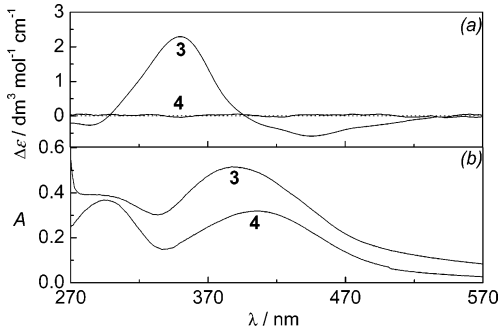

Figure 4. Circular dichroism (a) and absorption (b) spectra of **3** (1.0×10^{-2} g dm^{-3}) and **4** (1.4×10^{-2} g dm^{-3}) in DMF at 25 °C.

positive Cotton effect around 350 nm ($\Delta\epsilon$ = 2.29 dm^{-3} mol^{-1} cm^{-1}, in DMF) and a negative Cotton effect around 445 nm ($\Delta\epsilon$ = −0.58 dm^{-3} mol^{-1} cm^{-1}), while no signal was observed for **4**. According to the pioneering studies of Kajtár[34] and Nau[35] et al. on the ICD phenomena of cyclodextrin complexes, we deduce that the *o*-tolidine moiety of **1** is almost parallel to the axis of symmetry of the β-CD (that is, the axis of the cavity) to embed in the cavity, which is consistent with the crystal structure. In a similar way, the conformation of **2** is like to that of **1**. Furthermore, the ICD signal of polypseudorotaxane **3** is different from these of the inclusion complexes **1** and **2**, which is attributed to the C═N bond in **3**. Interestingly, the circular dichroism spectra of **1** and **2** showed the positive Cotton effect around 273 nm ($\Delta\epsilon$ = 0.59 dm^{-3} mol^{-1} cm^{-1}) and 262 nm ($\Delta\epsilon$ = 0.62 dm^{-3} mol^{-1} cm^{-1}) in DMF, respectively, indicating that the β-CD and *o*-tolidine **(**or *p*-phthaldehyde) could form the inclusion complexes in DMF to be consistent with above results.

XRD, **TG, and DTA**. The powder X-ray diffraction (XRD) patterns of **3** and **4** were obtained using a Rigaku D/max-2500 diffractometer with Cu Kα radiation. Except for the reflection appeared at 2θ = 8.9° (9.93 Å), 10.6° (8.37 Å), 12.5° (7.09 Å), 19.5° (4.56 Å), 22.8° (3.90 Å), and 25.7° (3.46 Å) in the XRD pattern of **3**, the characteristic reflection of the polyazomethine at 2θ = 13.3° (6.66 Å), 14.2° (6.22 Å), and 16.2° (5.48 Å) in **4** are presented obvious splits at 2θ = 13.4° (6.63 Å), 13.9° (6.37 Å), 14.6° (6.06 Å), 15.3° (5.77 Å), and 16.0° (5.52 Å) in **3**, which revealed that the presence of β-CD led to some difference but maintained the ordered structure. It is noteworthy that some diffraction peaks of **4** but are still recognizable in the diffraction patterns of **3**. It was suspected that some unthreaded **4** might have

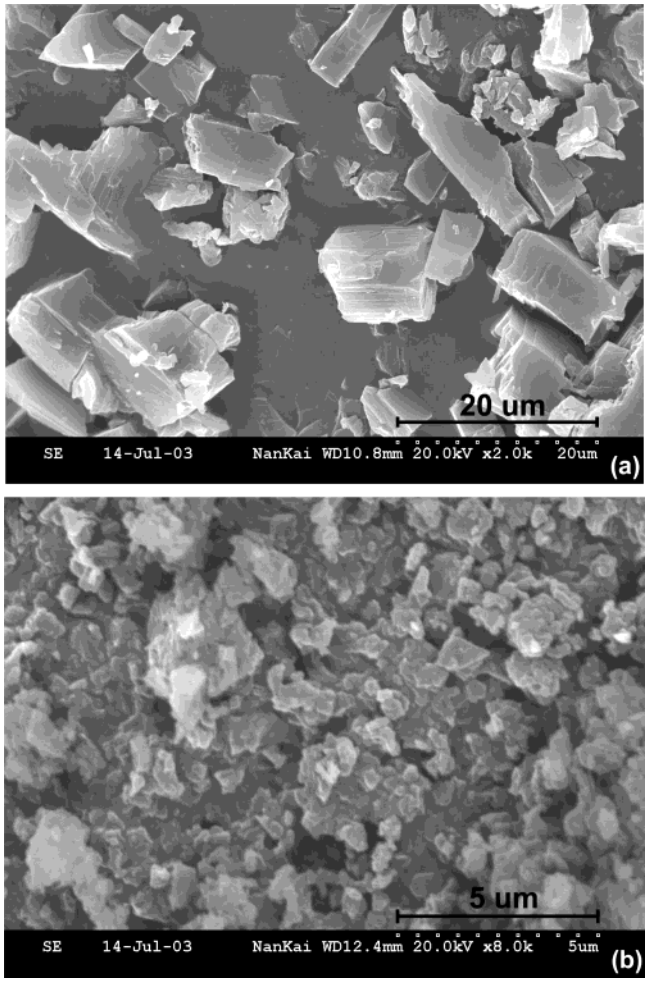

Figure 5. SEM images of (a) polypseudorotaxane **3** and (b) polyazomethine backbone **4**.

remained in **3**, so we washed **3** repeatedly with hot chloroform, in which **4** is sparingly soluble. Compared with the original diffraction pattern of **3**, the obtained diffraction pattern showed a little appreciable change upon washing with chloroform, and all those diffraction peaks representing **4** are similar in the two patterns. This result could exclude the existence of free unthreaded **4** in the compound **3**. One possible explanation for these results is that the chains of the conjugated **4** were rigid, so that the diffraction peaks in crystalline **4** phases was similar to those of unthreaded **4** in **3**.

To compare the thermal stabilities of **1**, **3**, and **4**, the thermogravimetric (TG) and differential thermal analysis (DTA) were recorded with a RIGAKU Standard type. Complex **1** starts losing weight at 296 °C and loses 83% of its original weight at 500 °C. Remarkably, **3** has two decomposition points of 253 and 446 °C, corresponding to the loss of β-CD and polyazomethine backbone, respectively, and loses 90% of its original weight at 600 °C. The decomposition point of **4** is at 407 °C, and 92.6% of its original weight is lost at 600 °C. The TG results show that though the decomposition point of **4** (407 °C) is higher than that of **1** (296 °C) and **3** (253 °C), the backbone decomposition point of **3** (446 °C) is higher than that of **4** (407 °C). DTA experiments have been performed and indicated that **1** displays an exothermic peak at 337 °C and **3** possesses an weak exothermic peak at 297 °C and an obvious exothermic peak at 574 °C, but **4** shows four exothermic peaks at 395, 488, 521, 532, and 550 °C. The higher thermal dissociation temperature for the backbone of **3** (574 °C) clearly indicates that β-CD plays a stabilizing role in the polypseudorotaxane.

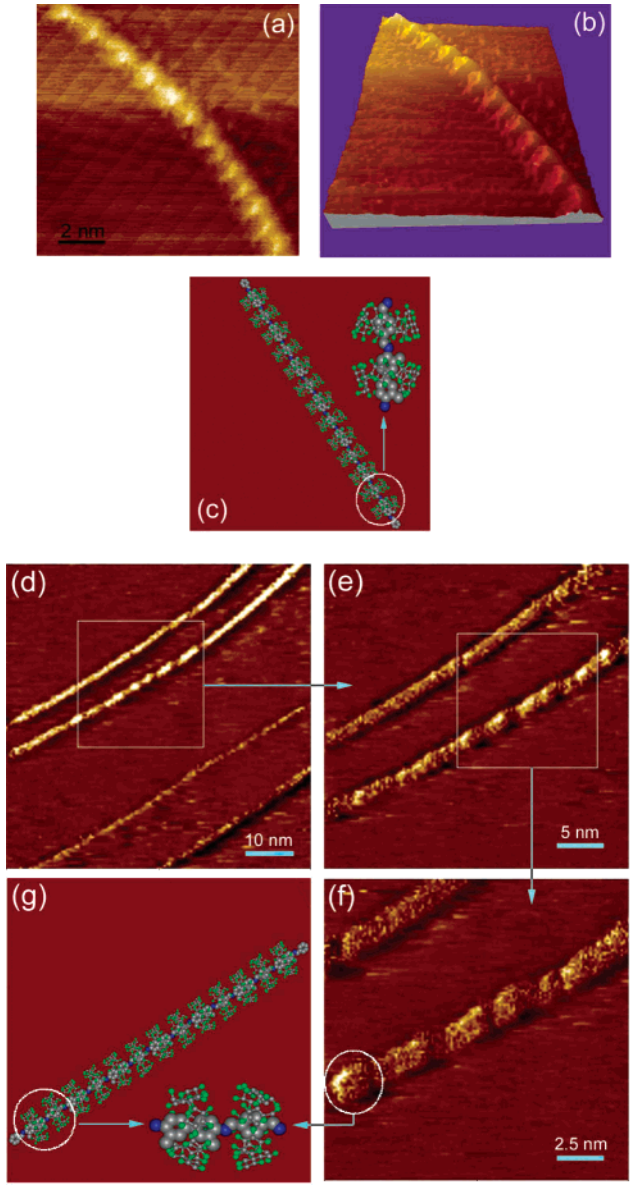

Figure 6. (a, d−f) STM images of the polypseudorotaxane **3** on a HOPG surface, (b) a 3D mode of STM image of the polypseudorotaxane **3**, and (c, g) the molecular modeling structures of **3**, which are omitted hydrogen atoms. The polypseudorotaxane is colored by atom type: blue, nitrogen atoms; green, oxygen atoms; gray, carbon atoms.

SEM and STM. To compare the surface morphologies of **3** and **4**, the scanning electron microscopy (SEM) experiments were performed. The SEM images in Figure 5 gave the macrostructure information about the polypseudorotaxane **3** and polyazomethine backbone **4**. Obviously, both **3** and **4** mainly showed the 3D regular structures, but the surface sizes of **4** are much smaller than that of **3**. Such difference in surface morphologies indicated that the presence of β-CDs changed the macrostructures of polypseudorotaxane **3**.

Scanning tunneling microscopy (STM) has become a convenient and widely employed method for the elucidation of the certain microstructures of the supramolecular aggregates.[36−40] For visualization, the STM experiments of **3** also were performed. A high-resolution STM image is shown in Figure 6a, from which it can be

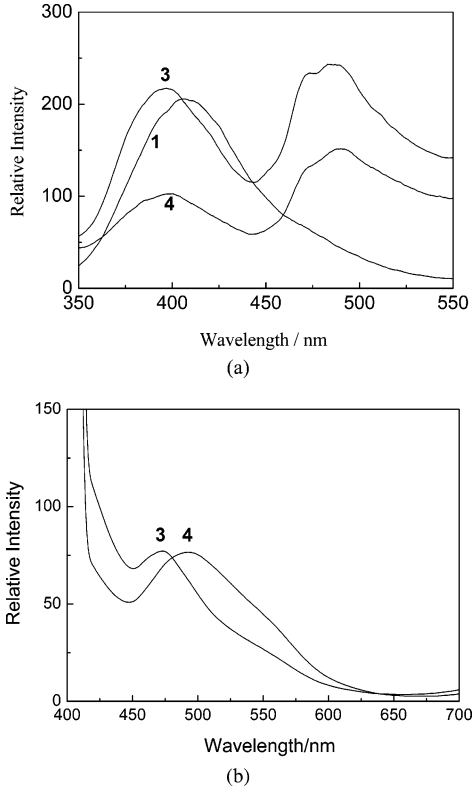

Figure 7. (a) Fluorescence spectra of **1** (2.0 × 10^{-6} mol dm^{-3}, in H_2O), **3** (1.0 × 10^{-2} g dm^{-3}, in DMF), and **4** (1.4 × 10^{-2} g dm^{-3}, in DMF) at 25 °C with an excitation wavelength of 290.0 nm. (b) Fluorescence spectra of **3** and **4** with an excitation wavelength of 400.0 nm at 25 °C.

seen that a nanometer-sized molecular wire with approximate 1.5 nm in diameter is distributed homogeneously on graphite (HOPG) substrate. Figure 6b gave a 3D mode of molecular wire with about 1.4 nm in height. Based on Figure 6a,b,d,e,f, Figure 6c,g showed the molecular modeling structures of **3** using WebLab ViewerPro 3.7 for Windows Molecular Modeling System. According to the size and shape, one bright dot in Figures 6a,b might correspond to a β-CD unit, which lies with longitudinal axes parallel to the HOPG surface. Because of the hydrogen-bonding interaction between the β-CDs,[38] longer chains that observed from STM experiments could be ascribed to intermolecular end-to-end association of these linear objects on HOPG surface.[17b,41] Nevertheless, the STM images provide direct evidence for the formation of the polypseudorotaxane **3**.

Optical Property and Fluorescence Lifetime. To display the photophysical behavior of **3** and **4**, their optical experiments were performed. The UV−vis absorption maxima of **1**, **2** (in H_2O), **3**, and **4** (in DMF) occurred at 280.4, 262.0, 387.5, and 405.5 nm, respectively. The emission spectrum (used a xenon lamp photosource) of **1** showed only a maximum at 406.0 nm, while **3** and **4** displayed two maximum peaks, at 397.0 and 483.0 nm for **3** and at 400.0 and 490.0 nm for **4** with an excitation wavelength of 290.0 nm (Figure 7a). It should be noted that the intensity of the emission peak of **3** at 483.0 nm is decreased ca. 30% after storing its saturated solution for 2 weeks, which means that the partially dissociation of **3** in DMF, so all optical experiments of **3** are performed by using the newly prepared solution. On the other hand, **3** and **4** in DMF under the excitation of wavelength of 400.0 nm showed

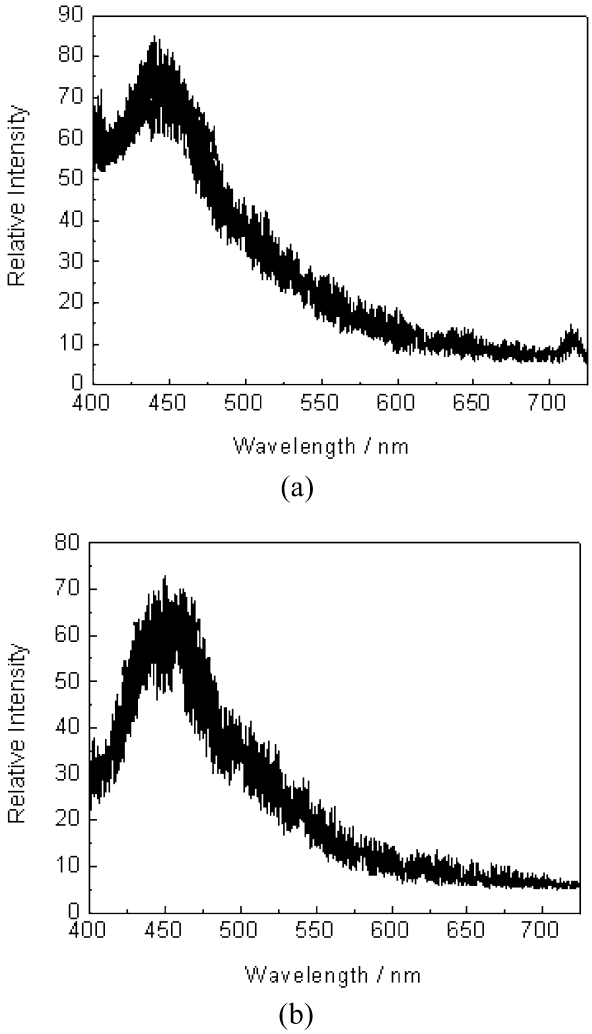

Figure 8. Photoluminescence spectra of (a) polypseudorotaxane **3** (1.0 × 10^{-2} g dm^{-3}) and (b) **4** (1.4 × 10^{-2} g dm^{-3}) in DMF at 25 °C with the excitation wavelength of 375.0 nm.

the maximum at 473.0 and 493.0 nm, respectively (Figure 7b).

Furthermore, the photoluminescence spectrum (used a laser photosource) of **4** dissolved in DMF showed a maximum peak at 450.3 nm with an excitation wavelength of 375.0 nm. Interestingly, polypseudorotaxane **3** gave two maximum peaks at 438.9 and 713.6 nm with same excitation wavelength (Figure 8). A possible explanation is that the polypseudorotaxane **3** possessing β-CDs as insulating layer could potential to eliminate the π-interactions of azomethine backbone and thereby dramatically increase the stability of molecular electronic materials.[17b] These results observed indicated that the samples **1**−**4** possess different photophysical behavior.

The inclusion complexation of fluorescent species by β-CD hosts not only induces the fluorescence enhancement and peak shifts but also leads to significantly elongated fluorescence lifetimes in the hydrophobic environment, as demonstrated by Bright[42] and Reinsborough.[43] In the present study, the nanosecond time-resolved fluorescence experiments of **3** and **4** are performed in DMF 25 °C, and the results obtained are summarized in Table 1.

Since the rates of complexation/decomplexation are much slower than that of the fluorescence decay, the decay profile of fluorescence intensity ($F(t)$) can be

Table 1. Fluorescence Lifetimes (τ) and Relative Quantum Yields (Φ) of 3 and 4 in DMF at 25 °C

	τ_S/ns	Φ_S/%	τ_L/ns	Φ_L/%
3	1.25	31.3	6.73	68.7
4	1.01	36.6	6.07	63.4

described as the sum of unimolecular decays for all fluorescing species present in the solution:

$$F(t) = \sum A_i \exp(-t/\tau_i) \quad (i = 1, 2, ...) \qquad (3)$$

where A_i and τ_i represent the initial abundance and lifetime of the ith species. As shown in Table 1, **3** and **4** gave a short lifetime (τ_S) and a long lifetime (τ_L), respectively, and the fluorescence lifetimes of **3** were longer than those of **4**, which indicated that the azomethine backbone of **3** is located in the β-CD hydrophobic cavity to show a longer lifetime. The experiments are in progress toward exploring the behavior of these new materials in the semiconductor and electroluminescent light-emitting diodes.

Conclusion

In conclusion, a nanometer-sized polypseudorotaxane **3** possessing β-CD as insulating layer is directly prepared by the polycondensation of two simple inclusion complexes, β-CD−*o*-tolidine complex **1** and β-CD−*p*-phthaldehyde complex **2**, displaying the different photophysical behavior as compared with the π-conjugated polyazomethine **4**. The present results prove not only a simple method for preparing insulated polypseudorotaxanes but also open a general access to designing versatile building units for more important potential in supramolecular science and polymer materials. Although these studies have focused on the assembly and properties of the polypseudorotaxane, the combination of these polymers with emerging methods could expect many more intriguing applications.

Experimental Section

Materials. β-CD of reagent grade (Shanghai Reagent Factory) was recrystallized twice from water and dried in vacuo at 95 °C for 24 h prior to use. *N*,*N*-Dimethylformamide (DMF) was dried over calcium hydride for 2 days and then distilled under a reduced pressure prior to use. 2,4-Dinitrofluorobenzene, *o*-tolidine, and *p*-phthaldehyde were commercially available and used without further purification.

Crystallography. The X-ray intensity data of **1** were collected on a standard Siemens SMART CCD area detector system equipped with a normal-focus molybdenum-target X-ray tube (λ = 0.710 73 Å) operated at 2.0 kW (50 kV, 40 mA) and a graphite monochromator at T = 293(2) K. The structures were solved by using direct method and refined by employing full-matrix least squares on F^2 (Siemens, SHELXTL, version 5.04).

CD, **UV−vis, and Fluorescence Spectra**. Circular dichroism (CD) and UV−vis spectra were recorded in a conventional quartz cell (light path 10 mm) on a JASCO J-715S spectropolarimeter or a Shimadzu UV-2401PC spectrophotometer equipped with a PTC-348WI temperature controller to keep the temperature at 25 °C. Fluorescence spectra were recorded in a conventional quartz cell (10 × 10 × 45 mm) at 25 °C on a JASCO FP-750 fluorescence spectrometer with the excitation and emission slits of 5 nm width.

SEM. A HITACHI S-3500N scanning electron microscopy (SEM) was used to take the SEM images.

STM. Scanning tunneling microscopy (STM) experiments were performed by using an Easyscan STM System with a Pt−Ir tip fabricated by Nanosurf AG of Switzerland and carried out with a sample bias voltage of +400 mV. All images were recorded in the constant-current mode at 3.0 nA. A DMF solution of sample **3** was prepared at a concentration of 1.0×10^{-2} g dm^{-3} and dripped onto a freshly prepared highly ordered pyrolytic graphite (HOPG) surface at room temperature. The sample was then dried in a vacuum for 3 h.

Complex 1. An ethanol solution (10 mL) of *o*-tolidine (1 mmol) was added dropwise to an aqueous solution (30 mL) of β-CD (1 mmol) and stirred at 40 °C for 5 h. The solvent was evaporated under a reduced pressure, and the precipitate formed was filtrated off to give a powder. The crude product was recrystallized from water and dried in vacuo to give **1** (yield 74%). A small amount of **1** was dissolved in hot water to make a saturated solution, which was then cooled to room temperature. After filtration, the resultant solution was kept at room temperature for about 2 weeks. The crystals formed were collected for X-ray crystallographic analysis.^{1}H NMR (300 MHz, D_2O, TMS, ppm): δ 2.04 (s, 6H), 3.35−3.63 (m, 42H), 4.81−4.82 (d, 7H), 6.61−6.64 (d, 2H), 6.91−6.94 (d, 4H). Anal. Calcd for $C_{56}H_{86}O_{35}N_2 \cdot 5H_2O$: C, 46.80; H, 6.73; N, 1.95. Found: C, 46.92; H, 6.75; N, 2.15.

Complex 2 was prepared from β-CD and *p*-phthaldehyde according to the procedure described above (yield 69%). ^{1}H NMR (300 MHz, D_2O, TMS, ppm): δ 3.32−3.75 (m, 42H), 4.83−4.85 (d, 7H), 7.92 (s, 4H), 9.86 (s, 2H). Anal. Calcd for $C_{50}H_{76}O_{37} \cdot 6H_2O$: C, 43.61; H, 6.44. Found: C, 43.67; H, 6.45.

Polypseudorotaxane 3. Complex **1** (0.4 mmol), β-CD (0.5 mmol), and $CaCl_2$ (0.3 mmol) were dissolved in 25 mL of DMF. A DMF solution (15 mL) of **2** (0.3 mmol) and β-CD (0.5 mmol) was then added dropwise to above solution and stirred at room temperature for 36 h under nitrogen. The solution turned yellow. Then, 2,4-dinitrofluorobenzene (0.05 mmol) was added dropwise to the solution and stirring continued for 24 h. The precipitate was filtered off to give a deep yellow powder. The polymers were washed repeatedly with DMF and methanol and dried in vacuo to give **3** (yield 37%). FTIR (KBr, cm^{-1}): ν 3361, 3022, 2919, 2879, 2733, 1622, 1541, 1517, 1481, 1432, 1336, 1303, 1204, 1156, 1125, 1031, 972, 945, 879, 832, 815, 741, 708, 581, 524, 450. ^{1}H MAS NMR (ppm): δ 2.70. ^{13}C CP/MAS NMR (ppm): δ 16.0, 19.8, 61.3, 73.6, 83.6, 103.4, 118.8, 125.8, 130.8, 139.4, 157.5. Powder X-ray diffraction (XRD): 2θ 8.9° (d 9.93 Å), 10.6 (8.37), 11.6 (7.60), 12.5 (7.09), 13.4 (6.63), 13.9 (6.37), 14.6 (6.06), 15.3 (5.77), 16.0 (5.52), 17.0 (5.20), 17.6 (5.02), 18.4 (4.83), 19.5 (4.56), 20.7 (4.28), 22.8 (3.90), 23.7 (3.74), 24.7 (3.60), 25.7 (3.46), 27.3 (3.27), 29.4 (3.03), 31.0 (2.88), 34.7 (2.58). Anal. Calcd for $C_{492}H_{722}O_{323}N_{14}$, n = 3 (MW: 12 001): C, 49.24; H, 6.06; N, 1.63. Found: C, 49.11; H, 5.87; N, 1.58.

Polymer 4. *o*-Tolidine (0.6 mmol) was dissolved in DMF (30 mL), and a DMF (20 mL) solution of *p*-phthaldehyde (0.5 mmol) was added dropwise. The resultant mixture was stirred at room temperature for 36 h under nitrogen and filtered off to give a yellow powder. The polymers were washed repeatedly with DMF and methanol followed by extraction with refluxing methanol in a Soxhlet apparatus for 5 h and dried in vacuo to give **4** (yield 83%). FTIR (KBr, cm^{-1}): ν 3341, 3103, 3030, 2949, 2918, 2871, 1621, 1590, 1517, 1428, 1336, 1277, 1229, 1185, 1144, 1125, 1062, 970, 924, 879, 832, 816, 743, 705, 523, 504, 450. ^{1}H MAS NMR (ppm): δ 2.47, 4.98, 7.59. ^{13}C CP/MAS NMR (ppm): δ 16.1, 20.2, 118.9, 127.5, 131.0, 139.3, 157.3, 160.9. Powder X-ray diffraction (XRD): 2θ 13.3° (d 6.66 Å), 14.2 (6.22), 16.2 (5.48), 17.6 (5.04), 18.3 (4.85), 20.6 (4.30), 23.7 (3.74), 24.6 (3.61), 26.8 (3.32), 27.4 (3.26), 29.3 (3.04). Anal. Calcd for $C_{168}H_{142}N_{16}$, n = 6 (MW: 2385): C, 84.60; H, 6.00; N, 9.40. Found: C, 84.31; H, 5.79; N, 9.36.

Acknowledgment. This work was supported by the NNSFC (No. 90306009, 20272028), Open Fund from State Key Laboratory of Functional Polymer Materials for Adsorption and Separation (No. 200304), and Special Fund for Doctoral Program from the Ministry of Education of China (No. 20010055001), which are gratefully acknowledged. We also thank the referees for their highly valuable suggestions regarding the revision.

Supporting Information Available: Molecular structure of complex **1**, ^{1}H NMR spectra, ^{13}C CP/MAS NMR spectra, ^{1}H MAS NMR spectra, FTIR spectra, powder X-ray diffraction, and TG-DTA. This material is available free of charge via the Internet at http://pubs.acs.org.

References and Notes

(1) (a) Nepogodiev, S. A.; Stoddart, J. F. *Chem. Rev.* **1998**, *98*, 1959−1976. (b) Raymo, F. M.; Stoddart, J. F. *Chem. Rev.* **1999**, *99*, 1643−1663.

(2) (a) Harada, A.; Li, J.; Kamachi, M. *Nature (London)* **1992**, *356*, 325−327. (b) Harada, A.; Li, J.; Kamachi, M. *Nature (London)* **1993**, *364*, 516−518. (c) Li, J.; Ni, X.; Leong, K. W. *Angew. Chem., Int. Ed.* **2003**, *42*, 69−72. (d) Li, J.; Ni, X.; Zhou, Z.; Leong, K. W. *J. Am. Chem. Soc.* **2003**, *125*, 1788−1795. (e) Okumura, H.; Kawaguchi, Y.; Harada, A. *Macromolecules* **2003**, *36*, 6422−6429.

(3) Li, G.; McGown, L. B. *Science* **1994**, *264*, 249−251.

(4) Craig, M. R.; Hutchings, M. G.; Claridge, T. D. W.; Anderson, H. L. *Angew. Chem., Int. Ed.* **2001**, *40*, 1071−1074.

(5) Wylie, R. S.; Macartney, D. H. *J. Am. Chem. Soc.* **1992**, *114*, 3136−3138.

(6) (a) Choi, H. S.; Huh, K. M.; Ooya, T.; Yui, N. *J. Am. Chem. Soc.* **2003**, *125*, 6350−6351. (b) Choi, H. S.; Ooya, T.; Sasaki, S.; Yui, N. *Macromolecules* **2003**, *36*, 5342−5347. (c) Huh, K. M.; Tomita, H.; Ooya, T.; Lee, W. K.; Sasaki, S.; Yui, N. *Macromolecules* **2002**, *35*, 3775−3777.

(7) (a) Liu, Y.; Li, L.; Zhang, H.-Y.; Zhao, Y.-L.; Wu, X. *Macromolecules* **2002**, *35*, 9934−9938. (b) Liu, Y.; You, C.-C.; Zhang, H.-Y.; Kang, S.-Z.; Zhu, C.-F.; Wang, C. *Nano Lett.* **2001**, *1*, 613−616. (c) Liu, Y.; Li, L.; Fan, Z.; Zhang, H.-Y.; Wu, X.; Liu, S.-X.; Guan, X.-D. *Nano Lett.* **2002**, *2*, 257−261.

(8) (a) Yamaguchi, I.; Osakada, K.; Yamamoto, T. *J. Am. Chem. Soc.* **1996**, *118*, 1811−1812. (b) Yamaguchi, I.; Osakada, K.; Yamamoto, T. *Macromolecules* **1997**, *30*, 4288−4294. (c) Yamaguchi, I.; Takenaka, Y.; Osakada, K.; Yamamoto, T. *Macromolecules* **1999**, *32*, 2051−2054. (d) Yamaguchi, I.; Osakada, K.; Yamamoto, T. *Macromolecules* **1997**, *33*, 2315−2319.

(9) (a) Rusa, C. C.; Fox, J.; Tonelli, A. E. *Macromolecules* **2003**, *36*, 2742−2747. (b) Abdala, A. A.; Tonelli, A. E.; Khan, S. A. *Macromolecules* **2003**, *36*, 7833−7841. (c) Shuai, X.; Porbeni, F. E.; Wei, M.; Bullions, T.; Tonelli, A. E. *Macromolecules* **2002**, *35*, 3126−3132.

(10) (a) Jiao, H.; Goh, S. H.; Valiyaveettil, S. *Macromolecules* **2002**, *35*, 1399−1402. (b) Jiao, H.; Goh, S. H.; Valiyaveettil, S. *Macromolecules* **2002**, *35*, 3997−4002.

(11) Gu, L.-Q.; Cheley, S.; Bayley, H. *Science* **2001**, *291*, 636−640.

(12) Shukla, A. D.; Bajaj, H. C.; Das, A. *Angew. Chem., Int. Ed.* **2001**, *40*, 446−448.

(13) Bong, D. T.; Clark, T. D.; Granja, J. R.; Ghadiri, M. R. *Angew. Chem., Int. Ed.* **2001**, *40*, 988−1011.

(14) Balzani, V.; Credi, A.; Raymo, F. M.; Stoddart, J. F. *Angew. Chem., Int. Ed.* **2000**, *39*, 3348−3391.

(15) Murakami, H.; Kawabuchi, A.; Kotoo, K.; Kunitake, M.; Nakashima, N. *J. Am. Chem. Soc.* **1997**, *119*, 7605−7606.

(16) Banerjee, I. A.; Yu, L.; Matsui, H. *J. Am. Chem. Soc.* **2003**, *125*, 9542−9543.

(17) (a) Taylor, P. N.; O'Connell, M. J.; McNeill, L. A.; Hall, M. J.; Aplin, R. T.; Anderson, H. L. *Angew. Chem., Int. Ed.* **2000**, *39*, 3456−3460. (b) Cacialli, F.; Wilson, J. S.; Michels, J. J.; Daniel, C.; Silva, C.; Friend, R. H.; Severin, N.; Samorì, P.; Rabe, J. P.; O'Connell, M. J.; Taylor, P. N.; Anderson, H. L. *Nature Mater.* **2002**, *1*, 160−164. (c) Michels, J. J.; O'Connell, M. J.; Taylor, P. N.; Wilson, J. S.; Cacialli, F.; Anderson, H. L. *Chem.*−*Eur. J.* **2003**, *9*, 6167−6176.

(18) Nepal, D.; Samal, S.; Geckeler, K. E. *Macromolecules* **2003**, *36*, 3800−3802.

(19) (a) Farcas, A.; Grigoras, M. *J. Optoelectron. Adv. Mater.* **2000**, *2*, 525−530. (b) Farcas, A.; Grigoras, M. *Polym. Int.* **2003**, *52*, 1315−1320.

(20) (a) Bredas, J. L., Chance, R. R., Eds. *Conjugated Polymeric Materials*: *Opportunity in Electronics, Optoelectronics, and Molecular Electronics*; Kluwer Academic Publishers: Dordrecht, Holland, 1990. (b) Skotheim, T. A., Ed. *Handbook of Conducting Polymers*; Marcel Dekker: New York, 1986. (c) Marder, S. R., Sohn, J. E., Stucky, G. D., Eds. *Materials for Nonlinear Optics: Chemical Perspectives*; American Chemical Society: Washington, DC, 1991.

(21) (a) Jenekhe, S. A.; Osaheni, J. A. *Science* **1994**, *265*, 765−768. (b) Yang, C.-J.; Jenekhe, S. A. *Chem. Mater.* **1991**, *3*, 878−887. (c) Yang, C.-J.; Jenekhe, S. A. *Chem. Mater.* **1994**, *6*, 196−203. (d) Yang, C.-J.; Jenekhe, S. A. *Chem. Mater.* **1995**, *7*, 1276−1285. (e) Yang, C.-J.; Jenekhe, S. A. *Macromolecules* **1995**, *28*, 1180−1196.

(22) Burroughes, J. H.; Bradley, D. D. C.; Brown, A. R.; Marks, R. N.; MacKay, K.; Friend, R. H.; Burn, P. L.; Holmes, A. B. *Nature (London)* **1990**, *347*, 539−541.

(23) Thomas, O.; Inganäs, O.; Andersson, M. R. *Macromolecules* **1998**, *31*, 2676−2678.

(24) Liu, Y.; Zhao, Y.-L.; Zhang, H.-Y.; Song, H.-B. *Angew. Chem., Int. Ed.* **2003**, *42*, 3260−3263.

(25) Crystal data for **1**: $C_{56}H_{102}N_2O_{43}$: $M_r = 1491.40$ (including water molecules); dimensions = 0.42 × 0.22 × 0.20 mm; orthorhombic; space group: *C*222(1); unit cell dimensions: $a = 19.347(5)$, $b = 24.266(6)$, $c = 32.806(6)$ Å, $V = 15401(6)$ Å^3; $\alpha = 90°$, $\beta = 90°$, $\gamma = 90°$; $Z = 8$; $\rho_{calcd} = 1.286$ g cm^{-3}; data/restraints/parameters 12942/125/791. Final R indices $R1 = 0.1355$, $wR2 = 0.3663$. CCDC-215569 contains the supplementary crystallographic data for this paper. These data can be obtained free of charge via www.ccdc.cam.ac.uk/conts/retrieving.html (or from the Cambridge Crystallographic Data Centre, 12, Union Road, Cambridge CB21EZ, UK.; fax (+44) 1223-336-033 or deposit@ccdc.cam.ac.uk).

(26) Meyer, E. A.; Castellano, R. K.; Diederich, F. *Angew. Chem., Int. Ed.* **2003**, *42*, 1210−1250.

(27) Kim, K. S.; Tarakeshwar, P.; Lee, J. Y. *Chem. Rev.* **2000**, *100*, 4145−4185.

(28) Harata, K. *Chem. Rev.* **1998**, *98*, 1803−1827.

(29) Sugiura, I.; Komiyama, M.; Toshima, N.; Hirai, H. *Bull. Chem. Soc. Jpn.* **1989**, *62*, 1643−1651.

(30) Harada, A.; Li, J.; Kamachi, M. *J. Am. Chem. Soc.* **1994**, *116*, 3192−3196.

(31) Hall, L. D.; Lim, T. K. *J. Am. Chem. Soc.* **1986**, *108*, 2503−2510.

(32) Gidley, M. J.; Bociek, S. M. *J. Am. Chem. Soc.* **1988**, *110*, 3820−3829.

(33) Cunha-Silva, L.; Teixeira-Dias, J. J. C. *J. Phys. Chem. B* **2002**, *106*, 3323−3328.

(34) Kajtár, M.; Horvath-Toro, C.; Kuthi, E.; Szejtli, J. *Acta Chim. Acad. Sci. Hung.* **1982**, *110*, 327−355.

(35) (a) Zhang, X.; Nau, W. M. *Angew. Chem., Int. Ed.* **2000**, *39*, 544−547. (b) Mayer, B.; Zhang, X.; Nau, W. M.; Marconi, G. *J. Am. Chem. Soc.* **2001**, *123*, 5240−5248.

(36) De Feyter, S.; Gesquiè, A.; Abdel-Mottaleb, M. M.; Grim, P. C. M.; De Schryver, F. C.; Meiners, C.; Sieffert, M.; Valiyaveettil, S.; Müllen, K. *Acc. Chem. Res.* **2000**, *33*, 520−531.

(37) Ohira, A.; Sakata, M.; Taniguchi, I.; Hirayama, C.; Kunitake, M. *J. Am. Chem. Soc.* **2003**, *125*, 5057−5065.

(38) Miyake, K.; Yasuda, S.; Harada, A.; Sumaoka, J.; Komiyama, M.; Shigekawa, H. *J. Am. Chem. Soc.* **2003**, *125*, 5080−5085.

(39) Tchebotareva, N.; Yin, X.; Watson, M. D.; Samorì, P.; Rabe, J. P.; Müllen, K. *J. Am. Chem. Soc.* **2003**, *125*, 9734−9739.

(40) Jeon, Y. J.; Bharadwaj, P. K.; Choi, S.; Lee, J. W.; Kim, K. *Angew. Chem., Int. Ed.* **2002**, *41*, 4474−4476.

(41) Liu, H.; Wang, S.; Luo, Y.; Tang, W.; Yu, G.; Li, L.; Chen, C.; Liu, Y.; Xi, F. *J. Mater. Chem.* **2001**, *11*, 3063−3067.

(42) Bright, F. V.; Catena, G. C. *Anal. Chem.* **1989**, *61*, 905−909.

(43) Jobe, D. J.; Verrall, R. E.; Paleu, R.; Reinsborough, V. C. *J. Phys. Chem.* **1988**, *92*, 3582−3586.

MA0356717